Nanoscale Res Lett (2009) 4:1275–1285
DOI 10.1007/s11671-009-9393-8

NANO EXPRESS

The Acute Liver Injury in Mice Caused by Nano-Anatase TiO_2

Linglan Ma · Jinfang Zhao · Jue Wang · Jie Liu · Yanmei Duan · Huiting Liu · Na Li · Jingying Yan · Jie Ruan · Han Wang · Fashui Hong

Received: 11 June 2009 / Accepted: 3 July 2009 / Published online: 1 August 2009

Abstract Although it is known that nano-TiO_2 or other nanoparticles can induce liver toxicities, the mechanisms and the molecular pathogenesis are still unclear. In this study, nano-anatase TiO_2 (5 nm) was injected into the abdominal cavity of ICR mice for consecutive 14 days, and the inflammatory responses of liver of mice was investigated. The results showed the obvious titanium accumulation in liver DNA, histopathological changes and hepatocytes apoptosis of mice liver, and the liver function damaged by higher doses nano-anatase TiO_2. The real-time quantitative RT-PCR and ELISA analyses showed that nano-anatase TiO_2 can significantly alter the mRNA and protein expressions of several inflammatory cytokines, including nucleic factor-κB, macrophage migration inhibitory factor, tumor necrosis factor-α, interleukin-6, interleukin-1β, cross-reaction protein, interleukin-4, and interleukin-10. Our results also implied that the inflammatory responses and liver injury may be involved in nano-anatase TiO_2-induced liver toxicity.

Keywords Mice · Nano-anatase TiO_2 · Liver · Inflammatory cytokines · Histopathological changes

Introduction

Titanium dioxide nanoparticles (nano-TiO_2) (<100 nm) are widely used in the cosmetics, pharmaceutical, and paint industries as a coloring material because of its high stability, anticorrosion, and photocatalysis. More and more nanoparticles are brought into the environment with the increasing development and application of nanotechnology. With the small size and large surface area, nanoparticles can be an active group or exert intrinsic toxicity. It is therefore important to clarify the effects of various nanoparticles on organs health as well as the pathogenic mechanisms involved.

This information may have important clinical implications regarding the safety issue, as nano-TiO_2 are widely used in the different spheres. Extra caution should therefore be taken in the handling of higher dose nano-TiO_2. Many in vivo studies showed that nanoparticles can be accumulated in the liver, kidney, spleen, lung, heart, and brain, whereby generating various inflammatory responses [1–8]. For instance, nanoparticles can promote enzymatic activities and the mRNA expression of cytokines during proinflammatory responses in rats and mice [5–8] and in human dermal fibroblasts and human lung epithelial cells [9]. In the study of toxicity of nano-TiO_2 to rats by intratracheal instillation, Afaq et al. [10] found that the number of alveolar macrophage increased, the activities of glutathione peroxidase, glutathione reductase, 6-phosphate glucose dehydrogenase, and glutathione *S*-transferase were significantly elevated. However, the production of lipid peroxidation and hydrogen peroxide radicals was not altered with increased activities of these enzymes, suggesting that nano-TiO_2 (<30 nm) could induce the generation of antioxidant enzymes in animals [10]. Oberdörster et al. [11] showed that the nano-TiO_2 (20 nm) induced the increase of the

Linglan Ma, Jinfang Zhao, and Jue Wang contributed equally to this work.

L. Ma · J. Zhao · J. Wang · J. Liu · Y. Duan · H. Liu · N. Li · J. Yan · J. Ruan · H. Wang · F. Hong (✉)
Medical College of Soochow University, 215123 Suzhou, People's Republic of China
e-mail: Hongfsh_cn@sina.com

total protein of bronchoalveolar lavage fluid and the activities of lactate dehydrogenase and acid-glucosidase in rats and mice. The toxic effects of nano-TiO_2 in adult mice have been accomplished, suggesting that higher dose nano-TiO_2 (25 and 80 nm) increased the ratio of alanine aminotransferase to aspartate aminotransferase, the activity of lactate dehydrogenase and the liver weight, and caused the hepatocyte necrosis [8]. Our previous reports indicated higher dose nano-anatase TiO_2 (5 nm) could damage liver function [12] and induced an oxidative attack in liver of mice [13].

It is well known that overexpression and activation of nucleic factor-κB (NF-κB) may contribute to the pathogenesis of hepatitis in animals [14]. Although it is known that nano-TiO_2 or other nanoparticles can induce serious liver toxicities, the mechanisms and the molecular pathogenesis are still unclear. For example, can nano-TiO_2 particles, which are similar to hepatovirus, bind to DNA and cause the inflammatory cascade after accumulation in liver? When nano-TiO_2 particles stimulate hepatocytes, can they induce inhibitory proteins such as IκBs phosphorylated and degraded, and then NF-κB activation, leading to the gene transcription of the proinflammatory cytokines and anti-inflammatory cytokines in the mouse liver?

Zhu et al. [15] proved that nano-TiO_2 of different size and types showed different extents of cytotoxicity on CHO cells and 293T cells with the sequence as 10–20 nm anatase > 50–60 nm anatase > 50–60 nm rutile. TiO_2 can be classified into three types: anatase, rutile, and amorphous. The photoactivity of anatase-type TiO_2 was greater than that of rutile, whereas amorphous do not show photocatalytic activity. Because anatase-type TiO_2 has the greatest toxicity to cells among the three types, we need further research to investigate its toxicity in mouse liver.

In this study, we investigate the effect of nano-anatase TiO_2 on the induction of liver toxicity and inflammatory response, its mechanisms, and the molecular pathogenesis. Our findings will provide an important theoretical basis for evaluating the toxicity underlying effects of nanoparticles on animals and human.

Materials and Methods

Chemicals and Preparation

Nano-anatase TiO_2 was prepared via controlled hydrolysis of titanium tetrabutoxide. The details of the synthesis are as follows [16]: Colloidal titanium dioxide was prepared via controlled hydrolysis of titanium tetrabutoxide. In a typical experiment, 1 mL of $Ti(OC_4H_9)_4$ dissolved in 20 mL of anhydrous isopropanol was added dropwise to 50 mL of double distilled water adjusted to pH 1.5 with nitric acid

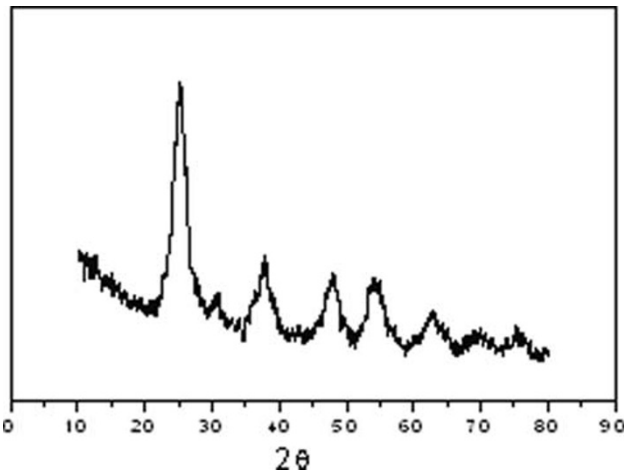

Fig. 1 The average grain size calculated from broadening of the (101) XRD peak of anatase using Scherrer's equation

under vigorous stirring at room temperature. Then, the temperature was raised to 60 °C and kept 6 h for better crystallization of nano-TiO_2 particles. The resulting translucent colloidal suspension was evaporated using a rotary evaporator yielding a nanocrystalline powder. The obtained powder was washed three times with isopropanol and dried at 50 °C until complete evaporation of the solvent. The average grain size calculated from broadening of the (101) X-ray diffraction peak of anatase (Fig. 1) using Scherrer's equation was approximately 5 nm. The Ti^{2+} content in the nano-anatase was measured by inductively coupled plasma mass spectroscopy (ICP-MS), and O, C, and H contents in the nano-anatase were assayed by Elementar Analysensysteme Gmbh, showing that Ti, O, C, and H contents in the nano-anatase were 58.114, 40.683, 0.232, and 0.136%, respectively. Bulk TiO_2 (rutile) was purchased from Shanghai Chem., Co., and the average grain size was 10–15 μm.

A 0.5% hydroxypropylmethylcellulose K4M (HPMC, K4M) was used as a suspending agent. Nano-anatase TiO_2 and bulk TiO_2 powder was dispersed onto the surface of 0.5%, w/v HPMC, and then the suspending solutions containing nano-TiO_2 and bulk TiO_2 particles were treated by ultrasonic for 30 min and mechanically vibrated for 5 min.

Animals and Treatment

CD-1 (ICR) mice of 70 females (20 ± 2 g) were purchased from the Animal Center of Soochow University. Animals were housed in stainless steel cages in a ventilated animal room. Room temperature was maintained at 20 ± 2 °C, with relative humidity at 60 ± 10%, and a 12-h light/dark cycle. Distilled water and sterilized food for mice were available ad libitum. They were acclimated to this environment for

5 days prior to dosing. All procedures used in animal experiments were in compliance with the local ethics committee. Animals were randomly divided into seven groups: control group (treated with 0.5% HPMC) and six experimental groups. Experimental groups were injected into abdominal cavity with nano-anatase TiO_2 (5, 10, 50, 100, and 150 mg/kg BW) and with bulk TiO_2 (150 mg/kg BW) everyday for 14 days, respectively. The control group was treated with 0.5% HPMC. The symptom and mortality were observed and recorded carefully everyday for 14 days. After 14 days, the body weight of all animals were weighed accurately and sacrificed after being anesthetized by ether. Blood samples were collected from the eye vein by removing the eyeball quickly. Serum was collected by centrifuging blood at 2,500 rpm for 10 min. The tissues and organs, such as liver, spleen, kidneys, lung, heart, and brain, were excised and washed carefully using 95% saline, then weighed accurately.

Coefficients of Liver

After weighing the body and tissues, the coefficients of liver to body weight were calculated as the ratio of tissues (wet weight, mg) to body weight (g).

Preparation of DNA Samples from Mouse Liver

The DNA was extracted from the liver and purified as described by the manual of DNA kits (Takara company), A260/A280 (>1.8) indicated that the DNA was sufficiently free of protein. The purified DNA was resuspended in Tris–HCl buffer (pH 7.2).

Titanium Content Analysis of Liver and Liver DNA

Tissues were taken out and thawed. About 0.1–0.3 g of each liver tissue and 0.5 mg of liver DNA from various treated mice were weighed, digested, and analyzed for titanium content. Briefly, prior to elemental analysis, the tissues of interest were digested in nitric acid (ultrapure grade) overnight. After adding 0.5 mL of H_2O_2, the mixed solutions were heated at about 160 °C using high-pressure reaction container in an oven chamber until the samples were completely digested. Then, the solutions were heated at 120 °C to remove the remaining nitric acid until the solutions were colorless and clear. At last, the remaining solutions were diluted to 3 mL with 2% nitric acid. ICP-MS (Thermo Elemental X7, Thermo Electron Co.) was used to analyze the titanium concentration in the samples. Of indium, 20 ng/mL was chosen as an internal standard element. The detection limit of titanium was 0.076 ng/mL. Data are expressed as nanograms per gram of fresh tissue.

Biochemical Analysis of Liver Function

Liver function was evaluated with serum levels of alanine aminotransferase (ALT), alkaline phosphatase (ALP), aspartate aminotransferase (AST), lactate dehydrogenase (LDH), pseudocholinesterase (PChE), leucine acid peptide (LAP), total protein, albumin (ALB), globulin (GLB), and total bilirubin (TBIL), triglycerides (TG), total cholesterol (TCHO), high-density lipoprotein cholesterol (HDL-C) and low-density lipoprotein cholesterol (LDL-C) using the commercial kits (Bühlmann Laboratories, Switzerland). All biochemical assays were performed using a clinical automatic chemistry analyzer (Type 7170A, Hitachi, Japan).

Histopathological Examination

For pathological studies, all histopathological tests were performed using standard laboratory procedures. The tissues were embedded in paraffin blocks, then sliced into 5 μm in thickness and placed onto glass slides. After hematoxylin–eosin (HE) staining, the slides were observed, and the photos were taken using optical microscope (Nikon U-III Multi-point Sensor System, USA), and the identity and analysis of the pathology slides were blind to the pathologist.

Observation of Hepatocyte Ultrastructure by TEM

Liver was fixed by 2.5% glutaraldehyde in 0.1 mol/dm^3 cacodylate buffer for 2 h, washed three times with 0.1 mol dm cacodylate buffer (pH 7.2–7.4) and post-fixed for 1 h in 1% osmium tetroxide. The specimens were dehydrated by a graded series of ethanol (75, 85, 95, and 100%) and embedded in Epon 812. Ultrathin sections were obtained, contrasted with uranyl acetate and lead citrate and observed with a JEOL 1010 transmission electron microscope.

Expression Amount and Concentration Assay of Inflammatory Cytokines

The mRNA expression of nucleic factor-κB (NF-κB), macrophage migration inhibitory factor (MIF), tumor necrosis factor-α (TNF-α), interleukin-6 (IL-6), interleukin-1β (IL-1β), cross-reaction protein (CRP), interleukin-4 (IL-4), and interleukin-10 (IL-10) were determined by real-time quantitative RT polymerase chain reaction (RT-PCR) [17–19]. Liver in the same growth period from the three different treatments were used. The right livers from mice with or without nano-anatase TiO_2 treatment were homogenized using QIAzol lysis reagent with a Tissue Ruptor (Roche). Total RNA from the homogenates was isolated using Tripure Isolation Reagent (Roche) according to the manufacturer's instructions. The RT reagent (Shinegene,

China) of 30 μL was prepared by mixing 15 μL of 2× RT buffer, 1 μL random primer in a concentration of 100 pmol μL^{-1}, 1 μL of RTase, 5 μL RNA, and 8 μL DEPC water together. The reaction condition was 25 °C for 10 min, 40 °C for 60 min, and 70 °C for 10 min.

Synthesized cDNA was used for the real-time PCR. Primers were designed using Primer Express Software according to the software guidelines.

The primer sequence is: Mnfkb1f: CATCCAACCTG AAAATCGTGAG, Mnfkb1r: CCCCAAATCCTTCCCA AACT, 156 bp; mil1bf: AAGTTGACGGACCCCAAA AG, mil1br: TGAGTGATACTGCCTGCCTGA, 129 bp; mtnff: TACTGAACTTCGGGGTGATCG, mtnfr: CCAC TTGGTGGTTTGCTACG, 156 bp; mil4f:TGTAGGGCTT CCAAGGTGCT, mil4r: TGATGCTCTTTAGGCTTTC CAG, 199 bp; mil6f: GTTGCCTTCTTGGGACTGATG, mil6r: ACTCTTTTCTCATTTCCACGATTT, 172 bp; mil10f: TGGACAACATACTGCTAACCGAC, mil10r: CCTGGGG CATCACTTCTACC, 111 bp; mcrpf: GCGGAAAAGTCTG-CACAAGG, mcrpr:GGAGATAGCACAAAGTCCCACAT, 153 bp; mmiff: CCATGCCTATGTTCATCGTGA, mmifr: ATCGTTCGTGCCGCTAAAAG, 167 bp; m actin f:GAGA-CCTTCAACACCCCAGC, m actin r: ATGTCACGCACGAT TTCCC, 263 bp.

All primers were purchased from Shinegene. For the 50 μL PCR reaction, 25 μL 2× PCR buffer, 0.6 μL 2× primers (25 pmol μL^{-1}), 0.3 μL probe (25 pmol μL^{-1}), 1 μL cDNA, and 22.8 μL DEPC water (Sigma) were mixed together. The parameters for a two-step PCR were 94 °C for 3 min, 94 °C for 20 s, 60 °C for 20 s, then 72 °C for 20 s, 35 cycles.

The gene expression analysis and experimental system evaluation were performed according to the standard curve and quantitation reports.

To determine NF-κB, MIF, TNF-α, IL-6, IL-1β, CRP, IL-4, and IL-10 levels of the plasma, enzyme linked immunosorbent assay (ELISA) was performed by using commercial kits that are selective for mouse NF-κB, MIF, TNF-α, IL-6, IL-1β, CRP, ILIL-4, and IL-10 (Biological Marker Laboratory, Inc., USA). Manufacturer's instruction was followed. The absorbance was measured on a microplate reader at 450 nm (Varioskan Flash, Thermo Electron, Finland) and the NF-κB, MIF, TNF-α, IL-6, IL-1β, CRP, IL-4, and IL-10 concentration of samples were calculated from a standard curve.

Statistical Analysis

Statistical analyses were done using SPSS11.5 software. Data were expressed as means ± SD. One-way analysis of variance (ANOVA) was carried out to compare the differences of means among multi-group data. Dunnett's test was carried out when each group of experimental data was compared with solvent-control data. Statistical significance for all tests was judged at a probability level of 0.05.

Results

The Enhancement of Body Weight and the Coefficients of Liver

After 14 days, the mice were weighed, various organs were collected and they were also weighed. Table 1 shows the coefficients of the liver to body weight which were expressed as milligrams (wet weight of tissues)/grams (body weight). No obvious differences were found in the body weight of seven groups. The significant differences were not observed in the coefficient of the liver in the 5 and 10 mg/kg BW nano-anatase TiO_2-treated groups ($p > 0.05$). However, the coefficients of the liver in the 50, 100, and 150 mg/kg BW nano-anatase TiO_2-treated groups and 150 mg/kg BW bulk TiO_2-treated group were significantly higher ($p < 0.05$ or 0.01) than the control, suggesting that higher dose nano-anatase TiO_2 and bulk TiO_2 might cause the damage of the liver of mice.

Titanium Contents in Liver and Liver DNA

The contents of titanium in liver and the purified DNA from liver of mice during 14 days daily injection of various doses nano-anatase TiO_2 and 150 mg/kg BW bulk TiO_2 are shown in Fig. 2. With increasing injection dose of nano-anatase

Table 1 The increase of net weight and coefficients of liver of mouse after intraperitoneal injection with nano-anatase TiO_2 suspensions for consecutive 14 days

Indexes	Nano-anatase (mg/kg BW)						Bulk (mg/kg BW)
	0	5	10	50	100	150	150
Net increase of BW (g)	7.35 ± 0.37	8.08 ± 0.40	7.82 ± 0.39	7.66 ± 0.38	7.27 ± 0.36	7.18 ± 0.36	7.36 ± 0.37
Liver/BW (mg/g)	56.81 ± 2.84	56.97 ± 2.85	60.09 ± 3.00	63.68 ± 3.18*	65.88 ± 3.29*	71.16 ± 3.58**	61.87 ± 3.09*

Ranks marked with an asterisk or double asterisks means it is significantly different from the control (no nano-anatase or bulk TiO_2) at the 5 or 1% confidence level, respectively. Values represent means ± SE, $n = 10$

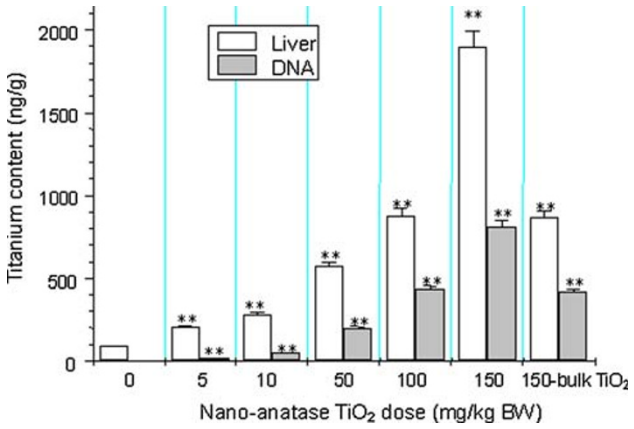

Fig. 2 The contents of titanium in liver tissue and liver DNA of female mouse after intraperitoneal injection with nano-anatase TiO_2 suspensions for consecutive 14 days. *Values* represent means ± SE, $n = 5$. *Columns* marked with *asterisk* or *double asterisks* means it is significantly different from the control (no nano-anatase or bulk-TiO_2) at the 5 or 1% confidence level, respectively

TiO_2, the titanium contents in the liver and DNA were significantly elevated, this observation suggested that the accumulation of titanium in the liver and DNA was closely related to the coefficients of the liver of mice, suggesting that, after entering the animals, nano-TiO_2 combine with the biomolecules such as DNA. However, the contents of titanium of the liver and DNA in 150 mg/kg BW bulk TiO_2-treated group were lower than those of 150 mg/kg BW nano-anatase TiO_2-treated group ($p < 0.05$), suggesting that nano-anatase TiO_2 entered the liver of mice and combined with the DNA more easily than the bulk TiO_2 did.

Assay of Liver Function

The serum biochemical parameters were assayed to further evaluate the toxicity of nano-anatase TiO_2 on the liver of mice. Table 2 exhibits the changes of biochemical parameters in serum of mice liver after nano-anatase TiO_2 suspension was injected into abdominal cavity for consecutive 14 days. In lower doses (5 and 10 mg/kg BW), there were no significant changes for all the parameters compared with the control group ($p > 0.05$). In higher dose of nano-anatase TiO_2-treated (50, 100, and 150 mg/kg BW) groups, however, the activities of ALT, ALP, AST, LDH, PChE, and LAP were significantly higher than the control group ($p < 0.05$ or 0.01), and the obvious enhancement of ALB, GLB levels, the reduction of ratio of ALB to GLB, TBIL levels were observed in comparison with the control group ($p < 0.05$). In the 150 mg/kg BW bulk TiO_2-treated group, there were only ALT, ALP, AST, LDH, PChE, and LAP higher than those of control ($p < 0.05$ or 0.01), and the other parameters had no obvious difference from the control group ($p > 0.05$). The increase of ALT, ALP, AST, LDH, PChE, and LAP, and the decrease of ratio of ALB to GLB, TBIL levels which are important indicators of the hepatic injury, demonstrated that nano-anatase TiO_2 induced hepatic injury. Furthermore, the increase of enzyme activity and the decrease of ratio of ALB to GLB, TBIL levels are dose-dependent, inferring that the induced hepatic injury is dose-dependent. TG, TCHO, and HDL-C from 100 to 150 mg/kg BW-treated groups were higher than the control group ($p < 0.05$). LDL-C contents from 100 to 150 mg/kg BW nano-anatase TiO_2 treated groups were lower than the control group ($p < 0.05$). In the 150 mg/kg BW bulk-TiO_2-treated group, the contents of THCO and HDL-C were higher than the control group ($p < 0.05$), but the contents of TG and LDL-C were not significantly different from the control group ($p > 0.05$). These results indicate that nano-anatase TiO_2 in higher dose caused metabolism imbalance of lipids HDL-C and low-density LDL-C in mice liver.

Liver Histopathological Evaluation

The histological photomicrographs of the liver sections are shown in Fig. 2. In the 5 mg/kg BW nano-anatase TiO_2-treated group, the liver tissue had no abnormal pathology changes compared with the control. In the 100, 150 mg/kg BW nano-anatase TiO_2-treated groups and 150 mg/kg BW bulk TiO_2-treated group, however, the significant histopathological changes were observed in the liver tissue, for example, congestion of vascellum and prominent vasodilatation were observed in 100 mg/kg BW nano-anatase TiO_2-treated group (Fig. 2c), and wide-bound basophilia and focal ischemia occurred in 150 mg/kg BW nano-anatase TiO_2-treated group (Fig. 2d, e), and congestion of central veins was showed in 150 mg/kg BW bulk TiO_2-treated group (Fig. 2f).

Hepatocyte Evaluation

Ultrastructure of hepatocyte in female mice is shown in Fig. 3. It was observed that the ultrastructure of hepatocyte from 5 mg/kg BW nano-anatase TiO_2-treated group was similar to the control, but from 100 mg/kg BW nano-anatase TiO_2-treated group turned tumescent mitochondria and vacuolization, and 150 mg/kg BW nano-anatase TiO_2-treated group indicated apoptotic body. The results suggested that nano-anatase TiO_2 could damage the structure of hepatocyte of mice.

Inflammatory Cytokines in Nano-Anatase TiO_2-Treated Mice Liver Tissues

The inflammation happened in liver according to the histopathological and hepatocyte ultrastructure observations. To confirm the role of inflammatory cytokine pathway in

Table 2 The changes of biochemical parameters in the blood serum of mouse liver after intraperitoneal injection with nano-anatase TiO_2 suspensions for consecutive 14 days

Indexes	Nano-anatase (mg/kg BW)						Bulk (mg/kg BW)
	0	5	10	50	100	150	150
ALT (U/L)	68.95 ± 3.45	72.66 ± 3.63	86.89 ± 0.34*	99.18 ± 4.96*	106.79 ± 5.34**	129.33 ± 6.47**	89.86 ± 4.49*
ALP (U/L)	208.59 ± 10.43	212.39 ± 10.62	234.72 ± 11.74	256.88 ± 12.84*	282.36 ± 14.12**	329.87 ± 16.49**	228.96 ± 11.45**
AST (U/L)	199.73 ± 9.99	210.47 ± 10.52	236.68 ± 11.83	268.92 ± 13.45**	297.55 ± 14.88**	345.88 ± 17.29**	246.78 ± 12.34**
LDH (U/L)	1,520 ± 76	1,623 ± 84	1,897 ± 95	2,318 ± 116*	2,689 ± 134**	2,949 ± 147**	2,309 ± 115*
PChE (U/L)	1,169 ± 58	1,297 ± 65	1,409 ± 70	1,696 ± 85*	1,988 ± 99**	2,597 ± 130**	1,647 ± 82*
LAP (U/L)	43.76 ± 2.19	47.25 ± 2.36	50.28 ± 2.51	56.81 ± 2.84*	60.19 ± 3.01*	63.66 ± 3.18*	52.72 ± 2.64*
TP (g/L)	60.15 ± 3.01	61.06 ± 3.05	62.59 ± 3.13	65.34 ± 3.27*	69.23 ± 3.46*	72.85 ± 3.64*	62.06 ± 3.10
ALB (g/L)	34.22 ± 1.71	34.30 ± 1.72	34.79 ± 1.74	35.92 ± 1.80	37.23 ± 1.86*	38.92 ± 1.95*	34.34 ± 1.72
GLB (g/L)	24.55 ± 1.23	24.98 ± 1.25	26.15 ± 1.31	27.44 ± 1.37*	30.15 ± 1.51*	33.57 ± 1.68**	25.05 ± 1.25
ALB/GLB	1.39	1.37	1.33	1.31*	1.24*	1.16**	1.37
TBIL (μmol/L)	1.35 ± 0.07	1.33 ± 0.07	1.29 ± 0.06	1.22 ± 0.06*	1.19 ± 0.06*	1.15 ± 0.06*	1.30 ± 0.06
TG (mmol/L)	1.66 ± 0.08	1.68 ± 0.08	1.72 ± 0.09	1.83 ± 0.09*	2.07 ± 0.10*	2.25 ± 0.11**	1.79 ± 0.09
TCHO (mmol/L)	3.19 ± 0.16	3.14 ± 0.16	3.21 ± 0.16	3.29 ± 0.16	3.51 ± 0.18*	3.66 ± 0.18*	3.57 ± 0.18*
HDLC (mmol/L)	2.86 ± 0.14	2.83 ± 0.14	2.91 ± 0.14	3.01 ± 0.15	3.34 ± 0.17*	3.52 ± 0.18*	3.36 ± 0.17*
LDLC (mmol/L)	0.26 ± 0.01	0.25 ± 0.01	0.22 ± 0.01	0.17 ± 0.01*	0.15 ± 0.01*	0.12 ± 0.01*	0.19 ± 0.01

Ranks marked with an asterisk or double asterisks means it is significantly different from the control (no nano-anatase or bulk TiO_2) at the 5 or 1% confidence level, respectively. Values represent mean ± SE, $n = 5$

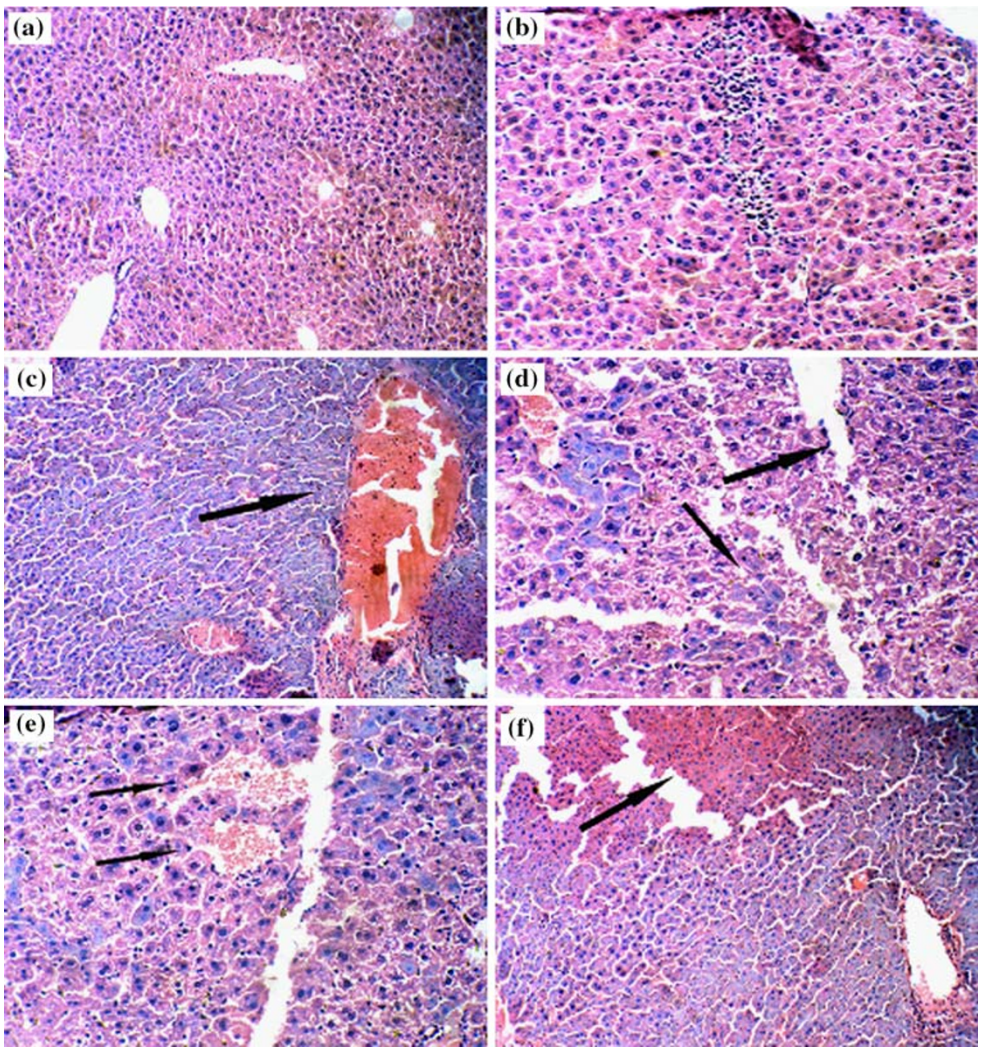

Fig. 3 Histopathology of the liver tissue (×100 or ×200) in female mice after intraperitoneal injection with various doses of nano-anatase TiO_2 suspensions for consecutive 14 days. **a** Control (×100): hepatocyte array is complete; **b** 5 mg/kg BW nano-anatase TiO_2 (×100): hepatocyte is normal, sinus hepaticus is complete, vascellum is normal; **c** 100 mg/kg BW nano-anatase TiO_2 (×100): *Arrows* indicate congestion of vascellum and prominent vasodilatation; **d** 150 mg/kg BW nano-anatase TiO_2 (×200): *Arrows* indicate wide-bound basophilia; **e** 150 mg/kg BW nano-anatase TiO_2 (×200): *Arrows* indicate focal ischemia; **f** 150 mg/kg BW bulk TiO_2 (×100): *Arrows* indicate congestion of central veins

nano-anatase TiO_2-induced liver injury, real-time quantitative RT-PCR, and ELISA were used to demonstrate inflammatory cytokines (such as NF-κB, MIF, IL-6, IL-1β, CRP, TNF-α, IL-4, and IL-10) induction in nano-anatase TiO_2-treated mice.

Real-time quantitative RT-PCR analysis showed that NF-κB, MIF, IL-1β, IL-6, CRP, TNF-α, IL-4, and IL-10 were significantly up-regulated in the liver tissues of mice treated with nano-anatase TiO_2 for consecutive 14 days ($p < 0.05$ or 0.01). The 150 mg/kg BW bulk TiO_2 microparticles (micro TiO_2) had less effect on induction of these genes compared with 150 mg/kg BW nano-anatase TiO_2 particles (Table 3).

The nano-anatase TiO_2-induced inflammatory cytokine expression was also examined at the protein level after intraperitoneal injection with various doses of nano-anatase TiO_2 suspensions for consecutive 14 days (Fig. 4). ELISA analysis showed that nano-anatase TiO_2 caused significant induction of serum levels of NF-κB, MIF, IL-6, IL-1β, CRP, TNF-α, IL-4, and IL-10 protein in a dose-dependent manner (Table 4, $p < 0.05$ or 0.01), which might be produced mainly by infiltrating macrophages and some liver epithelial cells.

The results mentioned earlier are consistent with that the histological photomicrograph and hepatocyte ultrastructure of the liver sections was observed in the treated mice. The inflammation is able to induce an increase of the expression level of inflammatory cytokines by nano-anatase TiO_2.

Discussion

The results of this study indicate that intraperitoneal injection of higher doses of nano-anatase TiO_2 can increase coefficients of the liver, and its significant accumulation in the mouse liver can induce histopathological changes of liver, including congestion of vascellum, prominent vasodilatation, wide-bound basophilia and focal ischemia, hepatocyte tumescent mitochondria, vacuolization and apoptosis, thus leading to the damage of liver function.

Table 3 Effects of nano-TiO_2 on the amplification of cytokine mRNA of mouse by real-time PCR analysis after intraperitoneal injection with nano-anatase TiO_2 suspensions for consecutive 14 days

Cytokine		Nano-anatase (mg/kg BW)				
		0	50	100	150	150-bulk
Refer-actin	Ct	21.035	19.93	21.4249	21.8257	21.038
	Copies	2.68E+07	5.64E+07	2.06E+07	1.57E+07	2.68E+07
nf-κb	Ct	23.144	21.7009	22.4526	22.2415	23.0754
	Relative copies	6.47E+06	1.71E+07	1.02E+07	1.19E+07	6.78E+06
	Ratio of *nf-κb*/actin	0.242 ± 0.012	0.303 ± 0.015*	0.497 ± 0.025**	0.756 ± 0.038**	0.253 ± 0.013
mif	Ct	22.4026	21.7153	21.5595	21.5625	20.5766
	Relative copies	1.07E+07	1.70E+07	1.88E+07	1.88E+07	3.65E+07
	Ratio of *mif*/actin	0.398 ± 0.020	0.634 ± 0.032**	0.913 ± 0.046**	1.194 ± 0.060**	0.647 ± 0.032**
il-1β	Ct	24.2684	22.911	20.9252	22.2075	24.0418
	Relative copies	3.04E+06	7.57E+06	2.89E+07	1.22E+07	3.54E+06
	Ratio of *il-1β*/actin	0.113 ± 0.006	0.481 ± 0.024**	0.511 ± 0.026**	0.590 ± 0.030**	0.132 ± 0.007*
il-6	Ct	25.076	22.6692	23.3343	22.8735	23.4873
	Relative copies	1.76E+06	8.9lE+06	5.70E+06	7.77E+06	5.14E+06
	Ratio of *il-6*/actin	0.066 ± 0.003	0.158 ± 0.008**	0.276 ± 0.014**	0.494 ± 0.025**	0.192 ± 0.010**
crp	Ct	23.9738	21.7188	23.152	22.907	23.0768
	Relative copies	3.70E+05	1.69E+07	6.44E+06	7.59E+06	6.77E+06
	Ratio of *crp*/actin	0.138 ± 0.007	0.300 ± 0.015**	0.312 ± 0.016**	0.482 ± 0.024**	0.253 ± 0.013**
tnf	Ct	28.674	28.8403	28.659	28.3492	28.7297
	Relative copies	1.56E+05	1.39E+05	1.58E+05	1.94E+05	1.50E+05
	Ratio of *tnf*/actin	0.028 ± 0.001	0.052 ± 0.003**	0.076 ± 0.004**	0.123 ± 0.006**	0.056 ± 0.003
il-4	Ct	23.7878	22.2796	21.1993	21.3352	22.906
	Relative copies	4.20E+06	1.16E+07	2.40E+07	2.19E+07	7.60E+06
	Ratio of *il-4*/actin	0.157 ± 0.008	0.205 ± 0.010**	0.895 ± 0.045**	1.392 ± 0.070**	0.369 ± 0.018**
π-10	Ct	28.5199	27.022	28.6367	28.1555	28.169
	Relative copies	173E+05	4.75E+05	1.60E+05	2.21E+05	2.19E+05
	Ratio of *π-10*/actin	0.065 ± 0.003	0.084 ± 0.004*	0.102 ± 0.005**	0.107 ± 0.005**	0.082 ± 0.004*

Ranks marked with an asterisk or double asterisks means it is significantly different from the control (no nano-anatase or bulk TiO_2) at the 5 or 1% confidence level, respectively. Values represent mean ± SE, $n = 5$

Wang et al. [8] observed that the hydropic degeneration around the central vein was prominent and the spotty necrosis of hepatocyte in the liver tissue of female mice post-exposure 2 weeks to the 5 g/kg BW 80 nm and fine TiO_2 particles, but did not observed significant histopathological change in liver tissues of mice exposed to the 5 g/kg BW 25 nm TiO_2 particles. The present study indicates that the hepatitis of mice is triggered by nano-anatase TiO_2 activation of inflammatory cytokines that resulted in disruption of liver tissue, and hepatocyte injury and apoptosis.

Alkaline phosphatase is mainly distributed in the liver, bone, and in bile duct, and ALT and AST exist in the liver, heart, and other organs. When the organs injured, the activities of ALP, ALT, and AST in serum would increase. It is well known that LDH is an important isoenzyme in glycolysis and glyconeogenesis and widely exists in the heart, liver, lung, and many other tissues. When the tissues are subjected to injury, LDH would leak into the serum of blood from organs or cells, which resulted in the increase of LDH activity and its isoenzyme in the corresponding organs. Pseudocholinesterase (PChE, acylcholine acyl hydrolase) has been found in many animal tissues, and it may function in the metabolism of lipids and low-density lipoprotein. When the liver is subjected to injury, PChE activity is significantly elevated, thus leading to the damage of the metabolism of lipids and low-density lipoprotein. In order to further study the biochemical mechanism of nano-anatase TiO_2 particles, the parameters for the damages of the liver function, and lipid contents in the blood were determined. The results showed that, in the 50, 100, and 150 mg/kg BW nano-anatase TiO_2-treated groups, the parameters for hepatic function including ALT, ALP, AST, LDH, LAP, PChE, TP, ALB, GLB, TBIL, TG, TCHO, and HDL-C increased greatly and LDL-C decreased significantly in blood ($p < 0.05$ or 0.01). However, the parameters mentioned earlier from the 5 and 10 mg/kg BW nano-anatase

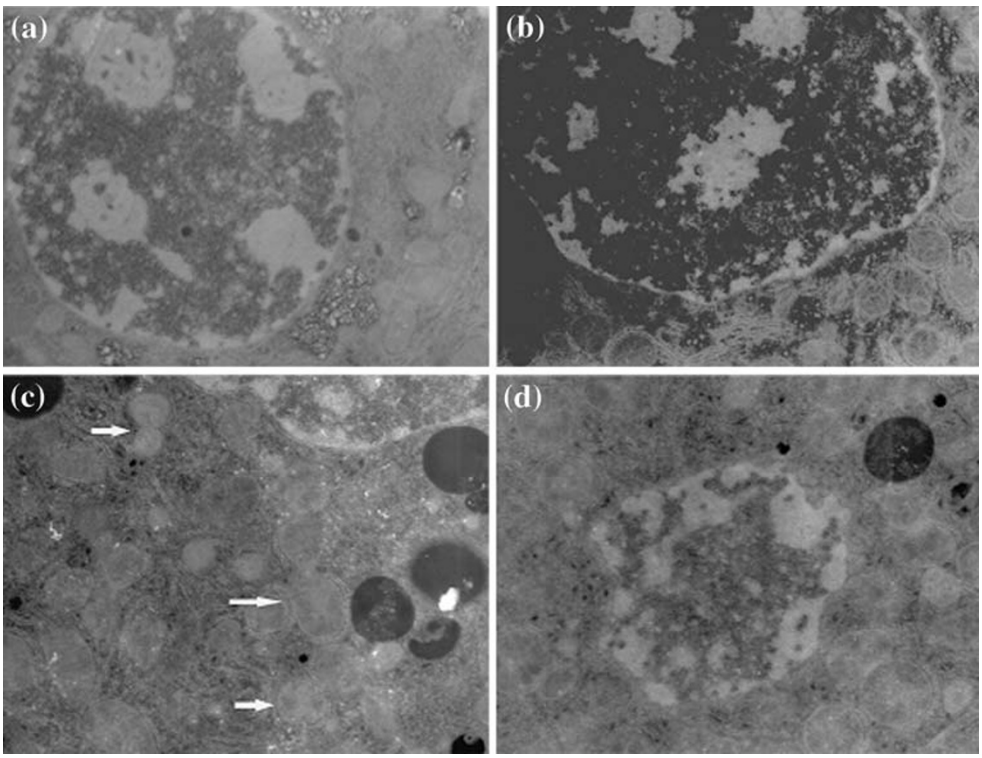

Fig. 4 Ultrastructure of hepatocyte (×8,000 or ×10,000) in female mice after intraperitoneal injection with various doses of nano-anatase TiO_2 suspensions for consecutive 14 days. **a** Control (×8,000): chromatin is well distributed, mitochondria turn round or oval and complete; **b** 5 mg/kg BW nano-anatase TiO_2 (×8,000): hepatocyte indicates normal; **c** 100 mg/kg BW nano-anatase TiO_2 (×10,000); *arrows* indicate tumescent mitochondria and vacuolization; **d** 150 mg/kg BW nano-anatase TiO_2 (×10,000): apoptotic cell or apoptotic body is observed

Table 4 Effects of nano-Tio_2 on the cytokine protein level of mice by ELISA analysis after intraperitoneal injection with nano-anatase TiO_2 suspensions for consecutive 14 days

Nano-anatase (mg/kg BW)	NF-κB (ng/mL)	MIF (pg/mL)	IL-1β (pg/mL)	IL-6 (pg/mL)	CRP (ng/mL)	TNF-α (pg/mL)	IL-4 (pg/mL)	IL-10 (pg/mL)
0	1,819 ± 91	1,157 ± 58	482 ± 24	179 ± 9	103 ± 5	156 ± 8	1,079 ± 54	615 ± 31
5	2,434 ± 122*	1,341 ± 67*	599 ± 30*	202 ± 10*	153 ± 8**	190 ± 10**	1,216 ± 61*	773 ± 39*
10	3,852 ± 193**	1,529 ± 76**	669 ± 34**	303 ± 15**	204 ± 0**	226 ± 11**	1,304 ± 65*	1,617 ± 81**
50	4,511 ± 226**	1,789 ± 89**	736 ± 37**	422 ± 21**	266 ± 13**	294 ± 15**	1,399 ± 70*	1,869 ± 94**
100	5,738 ± 287**	2,326 ± 116**	848 ± 42**	541 ± 27**	327 ± 16**	346 ± 17**	1,490 ± 75**	2,081 ± 104**
150	6,819 ± 341**	3,098 ± 155**	979 ± 49**	699 ± 35**	428 ± 21**	596 ± 30**	1,717 ± 86**	2,403 ± 120**
150-bulk	3,838 ± 192**	1,401 ± 70*	612 ± 31*	391 ± 20**	175 ± 9**	202 ± 10**	1,330 ± 67*	1,027 ± 51*

Ranks marked with a an asterisk or double asterisks means it is significantly different from the control (no nano-anatase or bulk TiO_2) at the 5 or 1% confidence level, respectively. Values represent mean ± SE, $n = 5$

TiO_2-treated groups were not significantly different from the control group. The results are consistent with histopathological changes of liver and the damage of hepatocyte substructure and with our previous report [12]. Wang et al. [8] showed that after a single oral gavage of dose of 5 g/kg BW of TiO_2 suspensions (25 and 80 nm), ALT, LDH, and TBIL in serum had statistical significance compared with the control mice.

Our studies showed that the obvious titanium accumulation in the liver and liver DNA of mice was observed. The accumulation of titanium is consistent with the coefficients of liver and the liver injury of mice. In addition, the accumulation of titanium of the organs in 150 mg/kg BW nano-anatase TiO_2-treated group was higher than those of 150 mg/kg BW bulk-TiO_2-treated group ($p < 0.05$). Compared with bulk TiO_2, smaller grain size of nano-

anatase TiO_2 (5 nm) would allow easier entry to mouse cells and its higher surface makes its intake to the liver and bound to liver DNA of mice easier. Combination of both resulted in the enhancement of the titanium in the liver and DNA. It implies that nano-TiO_2 particles, which are similar to hepatovirus, can enter liver cells or nuclei and bind to DNA, thus might cause the changes of genetic information transfer and the inflammatory cascade.

It is well known that the hepatitis pathogenesy is that hepatocytes generate various immunopathogenesis injuries, including cellular and humoral immunity. However, hepatovirus itself does not directly damage hepatocytes, some cytokines induced by hepatovirus play important roles in inflammatory responses. Transcription factor NF-κB is a critical intracellular mediator of the inflammatory cascade. In quiescent cells, NF-κB is bound to inhibitory proteins called IκBs that prevents NF-κB from migrating to the nucleus and located in the cytoplasm. When an appropriate inducer, such as hepatovirus, affects the cell, IκBs are phosphorylated and degraded, allowing nuclear uptake of NF-κB and initiating gene transcription (such as MIF, the proinflammatory cytokines of TNF-α, IL-6, IL-1β, CRP, and anti-inflammatory cytokines of IL-4 and IL-10) [14]. As an inflammatory factor, MIF also plays a role of inflammatory mediators in various diseases. The liver toxicity caused by nano-TiO_2 has been reported [8, 12], but its molecular pathogenesis is not known. In this study, the real-time quantitative RT-PCR and ELISA analysis showed that nano-anatase TiO_2 can significantly stimulate the mRNA expressions and increase protein levels of several inflammatory cytokines, including NF-κB, MIF, TNF-α, IL-6, IL-1β, CRP, IL-4, and IL-10. The obvious increase of these cytokines mRNA expression and protein levels indicated that the inflammatory responses and hepatocyte apoptosis may be involved in nano-anatase TiO_2-induced liver toxicity. It had been demonstrated that nano-TiO_2 could promote the expression of several cytokines and chemokines in the lung of rat and mice, including placenta growth factor (PlGF), MCP-1, IL-1β, and TNF-α [6, 20], and increase protein level of TNF-α, IL-1β in brain of mice and cause brain inflammation [21, 22]. Here, we speculate that nano-anatase TiO_2 particles, which are similar to hepatovirus, can make IκBs phosphorylated and degraded, and then induce NF-κB activation, leading to the expression of the NF-κB-controlled proinflammatory cytokines (such as IL-1β, IL-6) in liver of mice and the inflammatory response of liver, but the molecular mechanism of inflammatory response of mouse liver caused by nano-anatase TiO_2 needs to be studied in future. Further investigations are needed to elucidate the potential liver toxicity of different nanoparticles and their pathogenesis.

The present article also demonstrated that bulk-TiO_2 can elevate coefficients of the liver, be accumulated in liver and liver DNA of mice, cause histopathological changes of liver, damage liver function and induce inflammatory response of liver, but it has less toxicity compared with 150 mg/kg BW nano-anatase TiO_2 particles. Compared with nano-anatase TiO_2 (5 nm), bulk TiO_2, would allow hard entry to mouse cells and its lower surface makes its intake to the liver of mice hard.

Conclusion

The results of this study add our understanding of nano-anatase TiO_2-induced liver toxicity and inflammatory responses in liver of mice. Both are complicated multifactorial disease processes. We suggest that inflammatory cytokines cascade may cause inflammatory cell chemotaxis, and apoptosis, resulting in serious liver injury.

Acknowledgments This work was supported by the National Natural Science Foundation of China (grant no. 20671067), the Medical Development Foundation of Soochow University (grant no. EE120701) and the National Innovation Foundation of Student (grant no. 57315427, 57315927).

References

1. J.S. Brown, K.L. Zeman, W.D. Bennett, Am. J. Respir. Crit. Care Med. **166**, 1240 (2002)
2. W.G. Kreyling, M. Semmler, F. Erbe, P. Mayer, S. Takenaka, H. Schulz, G. Oberdorster, A. Ziesenis, J. Toxicol. Environ. Health A **65**, 1513 (2002)
3. G. Oberdoerster, Z. Sharp, V. Atudorei, A. Elder, R. Gelein, W. Kreyling, C. Cox, Inhal. Toxicol. **16**, 437 (2004)
4. G. Oberdörster, E. Oberdörster, J. Oberdörster, Environ. Health Perspect. **113**, 823 (2005)
5. J. Muller, F. Huaux, N. Moreau, P. Misson, J.F. Heilier, M. Delos, M. Arras, A. Fonseca, J.B. Nagy, D. Lison, Toxicol. Appl. Pharmacol. **207**, 221 (2005)
6. H.W. Chen, S.F. Su, C.T. Chien, W.H. Lin, S.L. Yu, C.C. Chou, J.W. Chen Jeremy, P.C. Yang, FASEB J. **20**, 2393 (2006)
7. T.T. Win-Shwe, D. Mitsushima, S. Yamamoto, A. Fukushima, T. Funabashi, T. Kobayashi, H. Fujimaki, Toxicol. Appl. Pharm. **226**, 192 (2008)
8. J.X. Wang, G.Q. Zhou, C.Y. Chen, H.W. Yu, T.C. Wang, Y.M. Ma, G. Jia, Y.X. Gao, B. Li, J. Sun, Y.F. Li, F. Jia, Y.L. Zhaso, Z.F. Chai, Toxicol. Lett. **168**, 176 (2007)
9. C.M. Sayes, R. Wahi, P.A. Kurian, Y.P. Liu, J.L. West, K.D. Ausman, D.B. Warheit, V.L. Colvin, Toxicol. Sci. **92**, 174 (2006)
10. F. Afaq, P. Abidi, R. Matin, Q. Rahman, J. Appl. Toxicol. **18**, 307 (1998)
11. G. Oberdörster, J.N. Finkelstein, C. Johnston, Res. Rep. Health Eff. Inst. **96**, 5 (2000)
12. H.T. Liu, L.L. Ma, J.F. Zhao, J. Liu, J.Y. Yan, J. Ruan, F.S. Hong, Biol. Trace Element Res. **129**(1), 170 (2009)
13. H.T. Liu, L.L. Ma, J.F. Zhao, J. Liu, J.Y. Yan, J. Ruan, F.S. Hong, Toxicol. Environ. Chem. (2009). doi: 10.1080/0277224 0902732530 (in press)
14. S. Ghosh, M.J. May, E.B. Kopp, Annu. Rev. Immunol. **16**, 225 (1998)

15. R.R. Zhu, S.L. Wang, J. Chao, D.L. Shi, R. Zhang, X.Y. Sun, S.D. Yao, Mater. Sci. Eng. C **29**, 691 (2009)
16. P. Yang, C. Lu, N. Hua, Y. Du, Mater. Lett. **57**, 794 (2002)
17. K.J. Livak, T.D. Schmittgen, Methods **25**, 402 (2001)
18. L.D. Ke, Z.A. Chen, Mol. Cell. Probes **14**(2), 127 (2000)
19. W.H. Liu, A. David, Biochem. Biophys. Res. Commun. **294**, 347 (2002)
20. D. Hohr, Y. Steinfartz, R.P. Schins, A.M. Knaapen, G. Martra, B. Fubini, P.J. Bor, Int. J. Hyg. Environ. Health **205**, 239 (2002)
21. J.X. Wang, Y. Liu, F. Jiao, F. Lao, W. Li, Y.Q. Gu, Y.F. Li, C.C. Ge, G.Q.B. Zhou, Y.L. Zhao, Z.F. Chai, C.Y. Chen, Toxicology **254**, 82 (2008)
22. J.X. Wang, C.Y. Chen, Y. Liu, F. Jiao, W. Li, F. Lao, Y.F. Li, B. Li, Y.Q. Gu, C.C. Ge, G.Q. Zhou, Y.X. Gao, Y.L. Zhao, Z.F. Chai, Toxicol. Lett. **183**, 72 (2008)